articles

molecular pharmaceutics

Targeted Delivery of Antisense Oligodeoxynucleotide by Transferrin Conjugated pH-Sensitive Lipopolyplex Nanoparticles: A Novel Oligonucleotide-Based Therapeutic Strategy in Acute Myeloid Leukemia

Yan Jin,[†,‡] Shujun Liu,[∥,⊥] Bo Yu,[†,§] Sharon Golan,[#] Chee-Guan Koh,[†,§] Jintao Yang,[†,§] Lenguyen Huynh,[∥,⊥] Xiaojuan Yang,[†,‡] Jiuxia Pang,[∥,⊥] Natarajan Muthusamy,[∥,⊥] Kenneth K. Chan,[‡,⊥] John C. Byrd,[∥,⊥] Yeshayahu Talmon,[#] L. James Lee,[*,†,§] Robert J. Lee,[*,†,‡,∥] and Guido Marcucci[*,∥,⊥]

NSF Nanoscale Science and Engineering Center, Division of Pharmaceutics, College of Pharmacy, Department of Chemical and Biomolecular Engineering, The Comprehensive Cancer Center, and Division of Hematology and Oncology, Department of Internal Medicine, The Ohio State University, Columbus, Ohio, and Technion-Israel Institute of Technology, Haifa, Israel

Received August 21, 2009; Revised Manuscript Received October 13, 2009; Accepted October 23, 2009

Abstract: Therapeutic use of oligodeoxynucleotides (ODNs) that hybridize to and downregulate target mRNAs encoding proteins that contribute to malignant transformation has a sound rationale, but has had an overall limited clinical success in cancer due to insufficient intracellular delivery. Here we report a development of formulations capable of promoting targeted delivery and enhanced pharmacologic activity of ODNs in acute myeloid leukemia (AML) cell lines and patient primary cells. In this study, transferrin (Tf) conjugated pH-sensitive lipopolyplex nanoparticles (LPs) were prepared to deliver GTI-2040, an antisense ODN against the R2 subunit of ribonucleotide reductase that has been shown to contribute to chemoresistance in AML. LPs had an average particle size around 110 nm and a moderately positive zeta potential at $\sim$ 10 mV. The ODN encapsulation efficiency of LPs was >90%. These nanoparticles could release ODNs at acidic endosomal pH and facilitate the cytoplasmic delivery of ODNs after endocytosis. In addition, Tf-mediated targeted delivery of GTI-2040 was achieved. R2 downregulation at both mRNA and protein levels was improved by 8-fold in Kasumi-1 cells and 2- to 20-fold in AML patient primary cells treated with GTI-2040-Tf-LPs, compared to free GTI-2040 treatment. Moreover, Tf-LPs were more effective than nontargeted LPs, with 10 to 100% improvement at various concentrations in Kasumi-1 cells and an average of 45% improvement at 3 μM concentration in AML patient primary cells. Treatment with 1 μM GTI-2040-Tf-LPs sensitized AML cells to the chemotherapy agent cytarabine, by decreasing its IC_{50} value from 47.69 nM to 9.05 nM. This study suggests that the combination of pH sensitive LP formulation and Tf mediated targeting is a promising strategy for antisense ODN delivery in leukemia therapy.

Keywords: Lipopolyplex nanoparticles; transferrin; GTI-2040; acute myeloid leukemia; antisense; oligodeoxynucleotides

1. Introduction

Acute myeloid leukemia (AML) is a heterogeneous, malignant disease of the hematopoietic system characterized by clonal accumulation and expansion of immature myeloid cells in the bone marrow (BM) and blood. Mutations and overexpression of genes involved in normal patterns of cellular differentiation, proliferation and apoptosis have been discovered and correlated with the pathogenesis and prognosis of this disease. Despite the progress in the understanding of the mechanisms underlying the initiation and main-

10.1021/mp900205r
Published on Web 10/23/2009

tenance of this disease, only approximately 40% of the treated younger patients (aged <60 years) and <10% of older patients (aged ≥60 years) achieve long-term remission.[1,2] Thus, the dismal outcome of most of the AML patients underscores a lack of significant advancements in the treatment of this disease and calls attention to the need for development of novel therapeutic strategies that specifically target abnormally functioning genes.

Cytarabine (Ara-C), a cytidine analogue, is a chemotherapy agent commonly included in treatment regimens for AML.[3,4] It is intracellularly converted into Ara-cytidine triphosphate (Ara-CTP) and competes with the endogenous deoxycytidine triphosphate (dCTP) for incorporation into newly synthesized DNA. Once incorporated into DNA, the triphosphate metabolite inhibits DNA polymerase thereby resulting in termination of the DNA strand elongation and eventually cell death.[5,6]

Recently, ribonucleotide reductase (RNR) inhibition has shown promises to increase the cytotoxic activity of Ara-C.[7] RNR is an enzyme that catalyzes reducing ribonucleotides into deoxyribonucleotides. RNR is composed of two subunits, R1 and R2. Expression of R2 increases dramatically in late G1/early S phase, when DNA replication occurs. When overexpressed in malignant cells, RNR increases the endogenous levels of deoxyribonucleotide triphosphate (dNTP) including dCTP that compete with Ara-C and other nucleoside analogues and prevent their DNA incorporation. Conversely, RNR inhibition produces an increase in Ara-CTP/dNTP ratio, thereby augmenting DNA incorporation of Ara-CTP,[8] and in turn enhancing cytotoxicity in proliferating malignant cells. Therefore, therapeutic strategies aimed to reduce the activity of RNR are currently being tested in the clinic with the goal of enhancing antitumor activities of nucleoside analogues.

We have recently completed a phase I study of GTI-2040, a 20-mer antisense oligodeoxyribonucleotide (ODN) that specifically hybridizes to the mRNA of the R2 subunit of RNR,[9] in combination with high-dose Ara-C in AML.[7] We showed that treatment with GTI-2040 is feasible, and combination with high-dose Ara-C appears to contribute to disease response. Although we observed downregulation at R2 mRNA and protein levels and correlation of these changes with disease response,[7] the efficiency of targeted R2 downregulation appeared to be ≤50% decrease in the baseline target levels following antisense exposure. Among other possible causes, we hypothesized that the low pharmacologic efficiency of GTI-2040 was due to obstacles in the ODN delivery process,[10,11] such as rapid clearance in blood circulation, poor cellular uptake, and lack of specific targeting of the "free" antisense.

* Corresponding authors. These three senior authors contributed equally to the work described herein. Guido Marcucci, M.D., Division of Hematology and Oncology, The Ohio State University, 898 Biomedical Research Center, 460 West 12th Avenue, Columbus, OH 43210. E-mail: Guido.Marcucci@osumc.edu. Phone: (614) 293-5738. Fax: (614) 293-7525. Robert J. Lee, Ph.D., Division of Pharmaceutics, College of Pharmacy, The Ohio State University, 542 Parks Hall, 500 West 12th Ave, Columbus, OH 43210. E-mail: lee.1339@osu.edu. Phone: 614-292-4172. Fax: 614-292-7766. L. James Lee, Ph.D., Department of Chemical and Biomolecular Engineering, The Ohio State University, 1012 Smith Lab, 174 West 18th Ave, Columbus, OH 43210. E-mail: leelj@chbmeng.ohio-state.edu. Phone: (614) 292-2408. Fax: (614) 292-8295.

† NSF Nanoscale Science and Engineering Center, The Ohio State University.

‡ Division of Pharmaceutics, College of Pharmacy, The Ohio State University.

|| The Comprehensive Cancer Center, The Ohio State University.

⊥ Division of Hematology and Oncology, Department of Internal Medicine, The Ohio State University.

§ Department of Chemical and Biomolecular Engineering, The Ohio State University.

Technion-Israel Institute of Technology, Haifa, Israel.

(1) Bloomfield, C. D.; Lawrence, D.; Byrd, J. C.; Carroll, A.; Pettenati, M. J.; Tantravahi, R.; Patil, S. R.; Davey, F. R.; Berg, D. T.; Schiffer, C. A.; Arthur, D. C.; Mayer, R. J. Frequency of prolonged remission duration after high-dose cytarabine intensification in acute myeloid leukemia varies by cytogenetic subtype. *Cancer Res.* **1998**, *58*, 4173–4179.

(2) Byrd, J. C.; Mrozek, K.; Dodge, R. K.; Carroll, A. J.; Edwards, C. G.; Arthur, D. C.; Pettenati, M. J.; Patil, S. R.; Rao, K. W.; Watson, M. S.; Koduru, P. R.; Moore, J. O.; Stone, R. M.; Mayer, R. J.; Feldman, E. J.; Davey, F. R.; Schiffer, C. A.; Larson, R. A.; Bloomfield, C. D. Pretreatment cytogenetic abnormalities are predictive of induction success, cumulative incidence of relapse, and overall survival in adult patients with de novo acute myeloid leukemia: results from Cancer and Leukemia Group B (CALGB 8461). *Blood* **2002**, *100*, 4325–4336.

(3) Estey, E. H. Therapeutic options for acute myelogenous leukemia. *Cancer* **2001**, *92*, 1059–1073.

(4) Gandhi, V.; Estey, E.; Du, M.; Nowak, B.; Keating, M. J.; Plunkett, W. Modulation of the cellular metabolism of cytarabine and fludarabine by granulocyte-colony-stimulating factor during therapy of acute myelogenous leukemia. *Clin. Cancer Res.* **1995**, *1*, 169–178.

(5) Gandhi, V.; Estey, E.; Keating, M. J.; Plunkett, W. Fludarabine potentiates metabolism of cytarabine in patients with acute myelogenous leukemia during therapy. *J. Clin. Oncol.* **1993**, *11*, 116–124.

(6) Gandhi, V.; Plunkett, W. Modulation of arabinosylnucleoside metabolism by arabinosylnucleotides in human leukemia cells. *Cancer Res.* **1988**, *48*, 329–334.

(7) Klisovic, R. B.; Blum, W.; Wei, X.; Liu, S.; Liu, Z.; Xie, Z.; Vukosavljevic, T.; Kefauver, C.; Huynh, L.; Pang, J.; Zwiebel, J. A.; Devine, S.; Byrd, J. C.; Grever, M. R.; Chan, K.; Marcucci, G. Phase I study of GTI-2040, an antisense to ribonucleotide reductase, in combination with high-dose cytarabine in patients with acute myeloid leukemia. *Clin. Cancer Res.* **2008**, *14*, 3889–3895.

(8) Iwasaki, H.; Huang, P.; Keating, M. J.; Plunkett, W. Differential incorporation of ara-C, gemcitabine, and fludarabine into replicating and repairing DNA in proliferating human leukemia cells. *Blood* **1997**, *90*, 270–278.

(9) Lee, Y.; Vassilakos, A.; Feng, N.; Lam, V.; Xie, H.; Wang, M.; Jin, H.; Xiong, K.; Liu, C.; Wright, J.; Young, A. GTI-2040, an antisense agent targeting the small subunit component (R2) of human ribonucleotide reductase, shows potent antitumor activity against a variety of tumors. *Cancer Res.* **2003**, *63*, 2802–2811.

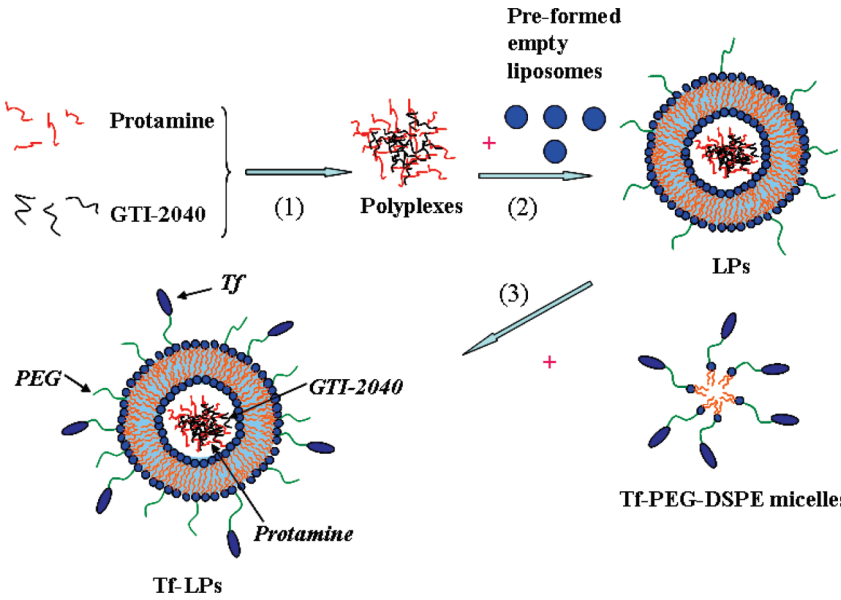

Figure 1. Schematic illustration for the preparation of LPs and Tf-LPs by ethanol dilution and postinsertion methods.

In this study, therefore, we utilized GTI-2040 to prove the principle that antisense delivery and antileukemic activity can be improved through newly devised formulations. We synthesized GTI-2040 transferrin (Tf)-conjugated PEGylated lipopolyplex nanoparticles (Tf-LPs) incorporating protamine as a DNA condensing agent, pH-sensitive fusogenic lipids to improve cytoplasmic delivery, and Tf as the targeting ligand specific for cellular delivery, which is commonly overexpressed on cancer cells including AML.[12,13] Using this delivery formulation, we showed that R2 downregulation at both mRNA and protein levels was significantly improved in AML cells treated with GTI-2040-Tf-LPs, compared to free GTI-2040 treatment.

2. Materials and Methods

2.1. Reagents. Dioleoyl phosphatidylethanolamine (DOPE) and distearoyl phosphatidylethanolamine-*N*-[maleimide-polyethylene glycol, MW 2000] (Mal-PEG$_{2000}$-DSPE) were purchased from Avanti Polar Lipids (Alabaster, AL). Methoxy-PEG$_{2000}$-DSPE was purchased from Genzyme Corporation (Cambridge, MA). Human holo-Tf, 2-iminothiolane (Traut's reagent), protamine sulfate, cholesteryl hemisuccinate (CHEMS), and other chemicals and reagents were purchased from Sigma Chemical Co. (St. Louis, MO). All tissue culture media and supplies were purchased from Invitrogen (Carlsbad, CA). All ODNs used in this study were fully phosphorothioated. GTI-2040 (sequence 5′-GGCTAAATCGCTCCACCAAG-3′) was generously supplied by Lorus Therapeutics Inc. (Toronto, Ontario, Canada). ODNs with scrambled sequence (5′-ACGCACTCAGCTAGTGACAC-3′) and carboxyfluorescein (FAM)-labeled GTI-2040 were purchased from Alpha DNA (Montreal, Quebec, Canada).

2.2. Cell Lines, Patient Samples and Cell Culture. Kasumi-1 and K562 cells were obtained from ATCC (Manassas, VA). Cells were grown in RPMI 1640 media supplemented with 10% (K562) or 15% (Kasumi-1) fetal bovine serum at 37 °C. Pretreatment unselected BM blasts from AML patients were obtained from OSU Leukemia Tissue Bank. Each of the patients signed an informed consent to storing and using his/her leukemia tissue for discovery studies according to institutional guidelines from OSU. Fresh AML primary BM samples were fractionated by Ficoll−Hypaque (Nygaard) gradient centrifugation and grown in RPMI 1640 media supplemented with 15% of human serum and GM-CSF plus Cytokine Cocktail (R&D Systems, MN) at 37 °C.

2.3. Preparation of Tf-LPs. As shown in Figure 1, an ethanol dilution method was used to prepare lipopolyplex nanoparticles (LPs) containing GTI-2040, scrambled ODNs or FAM-GTI-2040. Briefly, GTI-2040 ODNs were mixed with protamine in water at a 1:5 molar ratio for 30 min to form polyplexes. Meanwhile, a lipid mixture of DOPE/CHEMS/PEG-DSPE at a 58:40:2 molar ratio was dissolved in ethanol and then injected into 10 mM HEPES buffer, pH 8.0, to form empty liposomes in 10% ethanol. Then, preformed empty liposomes were mixed with the protamine/ODN suspension at a 12.5:1 lipid:ODN weight ratio, followed by vortexing and sonicating to spontaneously form LPs in the buffer solution. The final ethanol concentration

(10) Rait, A. S.; Pirollo, K. F.; Xiang, L.; Ulick, D.; Chang, E. H. Tumor-targeting, systemically delivered antisense HER-2 chemosensitizes human breast cancer xenografts irrespective of HER-2 levels. *Mol. Med.* **2002**, *8*, 475–486.
(11) Zhao, X. B.; Lee, R. J. Tumor-selective targeted delivery of genes and antisense oligodeoxyribonucleotides via the folate receptor. *Adv. Drug Delivery Rev.* **2004**, *56*, 1193–1204.
(12) Borhani, D. W.; Harrison, S. C. Crystallization and X-ray diffraction studies of a soluble form of the human transferrin receptor. *J. Mol. Biol.* **1991**, *218*, 685–689.
(13) Trowbridge, I. S.; Omary, M. B. Human cell surface glycoprotein related to cell proliferation is the receptor for transferrin. *Proc. Natl. Acad. Sci. U.S.A.* **1981**, *78*, 3039–3043.

in the cell culture was less than 1%. A postinsertion method was adopted to incorporate Tf ligand into ODN-loaded LPs.[14−17]

2.4. Cryogenic Transmission Electron Microscopy (Cryo-TEM). Cryo-TEM imaging was performed at Technion-Israel Institute of Technology, Haifa, Israel, as previously described.[18] Briefly, samples were examined in a Philips CM120 microscope (Eindhoven, The Netherlands) at 120 kV, using an Oxford CT-3500 cooling holder and transfer station (Abingdon, England). Specimens were equilibrated in the microscope below −178 °C, then examined in the low-dose imaging mode to minimize electron beam radiation damage, and recorded at a nominal underfocus of 1−2 μm to enhance phase contrast. Images were acquired digitally by a Gatan MultiScan 791 cooled charge-coupled device camera (Pleasanton, CA) using the Digital Micrograph 3.1 software package.

2.5. Characterization of LPs and Evaluation of ODN Encapsulation Efficiency. The particle size of LPs was analyzed on a NICOMP Particle Sizer model 370 (Particle Sizing Systems, Santa Barbara, CA). The volume-weighted Gaussian distribution analysis was used to determine the mean vesicle diameter. The zeta potential was determined on a ZetaPALS (Brookhaven Instruments Corp., Worcestershire, NY). All measurements were carried out in triplicate. The ODN encapsulation efficiency of LPs was determined using gel electrophoresis. First, LPs were lysed with 0.5% SDS and 1% Triton X-100, followed by agarose gel electrophoresis to separate SDS, Triton, and ODNs. Meanwhile, a series of ODN standards ($n = 5$) were loaded onto the agarose gel. The brightness and the expected amount of ODN of each band showed a linear correlation (correlation coefficient, $R^2 = 0.99$). Using this standard curve, the amount of ODN encapsulated in the LPs was then estimated by measuring the brightness of the ODN band. Encapsulation efficiency was calculated based on the ratio of ODNs in LPs versus the initial amount of ODNs applied. This method was validated for ODN quantification with the coefficient of variation less than 5% in three repeated experiments.

2.6. Study of Tf Receptor (TfR) Expression. The expression levels of TfR (also known as CD71) on the surface of AML cells were evaluated by surface staining with PE-labeled anti-TfR (anti-CD71) monoclonal antibodies (BD Biosciences, San Jose, CA) followed by flow cytometry analysis as previously described.[15] The details are explained in the Supporting Information.

2.7. Transfection Studies. Kasumi-1 and K562 cells were seeded at 5×10^5/mL density 24 h before transfection, while patient primary cells were seeded at 3×10^6/mL density right after they were separated from patient BM. During the transfection, cells were exposed to LPs, Tf-LPs or free ODNs at a final concentration of 1 μM or 3 μM. In "Mock" samples, cells were treated with 10 mM HEPES buffer. After 48 h, cells were collected and analyzed for *R2* mRNA level by real-time quantitative RT-PCR and for R2 protein level by Western blot.

2.8. Laser-Scanning Confocal Microscopy. Binding and internalization of FAM-GTI-2040-Tf-LPs in AML cells were examined by laser scanning confocal microscopy. Cells were incubated with FAM-GTI-2040-Tf-LPs for 0 h and 4 h respectively at 37 °C and washed twice with PBS followed by fixation with 2% para-formaldehyde for 30 min. Nuclei were stained with 20 μM DRAQ5 (Biostatus Limited, Leicestershire, U.K.) for 5 min at room temperature. The cells were mounted on a poly-D-lysine coated cover glass slide (Sigma-Aldrich, St. Louis, MO). Green fluorescence of FAM-GTI-2040 and blue fluorescence of DRAQ5 were acquired, and merged images were produced by using Zeiss 510 META laser scanning confocal imaging systems and LSM Image software (Carl Zeiss MicroImaging, Inc., NY).

2.9. Quantitative RT-PCR (qRT-PCR). The *R2* mRNA level in AML cells was evaluated using qRT-PCR as previously described.[19] Primer sequences for *R2* and *ABL*, and qRT-PCR conditions are reported in the Supporting Information.

2.10. Western Blot Analysis. The R2 protein expression was measured by Western blot as previously described.[20] Anti-R2 and anti-GAPDH antibodies were purchased from Santa Cruz Biotechnology (Santa Cruz, CA).[9] Equivalent gel loading was confirmed by probing with antibodies against GAPDH.

(14) Lopes de Menezes, D. E.; Pilarski, L. M.; Allen, T. M. In vitro and in vivo targeting of immunoliposomal doxorubicin to human B-cell lymphoma. *Cancer Res.* **1998**, *58*, 3320–3330.

(15) Lapalombella, R.; Zhao, X.; Triantafillou, G.; Yu, B.; Jin, Y.; Lozanski, G.; Cheney, C.; Heerema, N.; Jarjoura, D.; Lehman, A.; Lee, L. J.; Marcucci, G.; Lee, R. J.; Caligiuri, M. A.; Muthusamy, N.; Byrd, J. C. A novel Raji-Burkitt's lymphoma model for preclinical and mechanistic evaluation of CD52-targeted immunotherapeutic agents. *Clin. Cancer Res.* **2008**, *14*, 569–578.

(16) Schiffelers, R. M.; Ansari, A.; Xu, J.; Zhou, Q.; Tang, Q.; Storm, G.; Molema, G.; Lu, P. Y.; Scaria, P. V.; Woodle, M. C. Cancer siRNA therapy by tumor selective delivery with ligand-targeted sterically stabilized nanoparticle. *Nucleic Acids Res.* **2004**, *32*, e149.

(17) Chiu, S. J.; Liu, S.; Perrotti, D.; Marcucci, G.; Lee, R. J. Efficient delivery of a Bcl-2-specific antisense oligodeoxyribonucleotide (G3139) via transferrin receptor-targeted liposomes. *J. Controlled Release* **2006**, *112*, 199–207.

(18) Weisman, S.; Hirsch-Lerner, D.; Barenholz, Y.; Talmon, Y. Nanostructure of cationic lipid-oligonucleotide complexes. *Biophys. J.* **2004**, *87*, 609–614.

(19) Marcucci, G.; Livak, K. J.; Bi, W.; Strout, M. P.; Bloomfield, C. D.; Caligiuri, M. A. Detection of minimal residual disease in patients with AML1/ETO-associated acute myeloid leukemia using a novel quantitative reverse transcription polymerase chain reaction assay. *Leukemia* **1998**, *12*, 1482–1489.

(20) Liu, S.; Liu, Z.; Xie, Z.; Pang, J.; Yu, J.; Lehmann, E.; Huynh, L.; Vukosavljevic, T.; Takeki, M.; Klisovic, R. B.; Baiocchi, R. A.; Blum, W.; Porcu, P.; Garzon, R.; Byrd, J. C.; Perrotti, D.; Caligiuri, M. A.; Chan, K. K.; Wu, L. C.; Marcucci, G. Bortezomib induces DNA hypomethylation and silenced gene transcription by interfering with Sp1/NF-kappaB-dependent DNA methyltransferase activity in acute myeloid leukemia. *Blood* **2008**, *111*, 2364–2373.

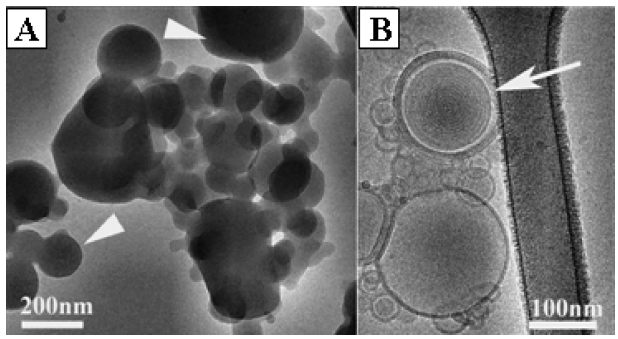

Figure 2. Cryo-TEM micrographs of polyplexes and LPs. (A) Amorphous complexes (arrowheads) of protamine/ODN; their internal structure is not visible. (B) White arrow shows the onion-like structure of LPs.

2.11. Cell Survival Studies by MTS Assay. Kasumi-1 cells were treated with HEPES buffer (as Mock), GTI-2040-Tf-LPs, free GTI-2040 or Scrambled-Tf-LPs at 1 μM concentration for 4 h and then incubated with various concentrations of Ara-C (0.0001−10 μM) for 48 h. Cell survival was then determined by treating with MTS (3-(4,5-dimethylthiazol-2-yl)-5-(3-carboxymethoxyphenyl)-2-(4-sulfophenyl)-2H-tetrazolium), which is reduced by cells into a formazan product that is soluble in tissue culture medium. Briefly, 20 μL of MTS/PMS (phenazine methosulfate) (ratio 20:1) mixture was added into each well and then incubated for 1−4 h at 37 °C. Absorbance was read at 490 nm on a microplate reader Germini XS (Molecular Devices, Sunnyvale, CA). Three replicates were tested at each drug concentration. Data were plotted and IC_{50} values were calculated using WinNonLin software (version 4.0, Pharsight, Mountain View, CA).

2.12. Statistical Analysis. Data were represented as mean ± standard deviations and analyzed by 2-tailed Student's *t* test using MiniTAB Program (Minitab Inc., State College, PA). $p < 0.05$ was considered statistically significant.

3. Results

3.1. Preparation and Characterization of LPs and Tf-LPs. In order to improve the delivery and efficacy of GTI-2040, we synthesized Tf-LPs. This process is schematically illustrated in Figure 1. Three steps were involved in the whole process: (1) Negatively charged GTI-2040 ODNs were condensed with positively charged protamine at 1:5 molar ratio in H_2O to synthesize a polyplex nano core; (2) the polyplex nano core was then mixed with negatively charged anionic liposomes to form LPs; (3) LPs were modified with Tf-PEG-DSPE micelles, previously synthesized as described,[14−17] to form the final Tf-LPs targeted nanoparticles that were used for the subsequent experiments.

The nanostructures of primary components of the Tf-LP targeted nanoparticles, the polyplexes synthesized in stage 1 (Figure 2A) and the LPs (Figure 2B) synthesized in stage 2, were then studied by direct nanoscale imaging via Cryo-TEM (Figure 2). Several coexisting structures were observed, including onion-like LPs (Figure 2B). LPs had an average particle size of 108.5 ± 5.4 nm and a zeta potential of 12.12 ± 0.82 mV. The GTI-2040 encapsulation efficiency of LPs was determined by agarose gel electrophoresis and found to be over 90% (Figure S1 in the Supporting Information).

3.2. TfR Expression on AML Cells and Patient Primary Cells. Tf is the targeting molecule on Tf-LPs, which can be efficiently taken up by cells expressing TfR via TfR-mediated endocytosis.[21,22] TfR is a dimeric transmembrane glycoprotein commonly overexpressed on proliferating cells including most tumor cells.[12,13] The expression of TfR on the surface of AML cells was studied using PE-labeled anti-TfR monoclonal antibodies. Kasumi-1 cells, K562 cells and AML patient primary cells that were used in this study demonstrated high levels of cell surface TfR expression (Figure 3A). The expression levels of TfR on Kasumi-1, K562 and patient primary cells were further increased by pretreatment with deferoxamine (DFO) (Figure 3A), an iron chelator known to increase TfR expression.[23]

3.3. Intracellular Uptake of GTI-2040-Tf-LPs. In order to study the uptake of GTI-2040-Tf-LPs, AML cells were treated with Tf-LPs containing FAM-labeled GTI-2040. The treated AML cells were harvested at various time points. Flow cytometry analysis of Tf-LPs containing FAM-labeled GTI-2040-treated cells evidenced a time-dependent increase in fluorescence signals (Figure 3B). The mean fluorescence intensity increased with time, as 9.4, 12.6, 29, 74.5 at 0 h, 15 min, 1 h and 4 h, respectively. The intracellular delivery of FAM-GTI-2040 into AML cells by Tf-LPs was confirmed with confocal microscopy (Figure 3C).

3.4. R2 Downregulation by GTI-2040-Tf-LPs in AML Cells. Having attained an efficient intracellular delivery of the antisense, next we tested whether this also resulted in downregulation of the R2 target at both mRNA and protein levels. In Kasumi-1 cells, we observed 23 ± 3% of R2 protein downregulation in cells treated with 1 μM of GTI-2040-Tf-LPs, while only approximately 10% downregulation or no changes were observed in cells treated with the nontargeted GTI-2040-LPs, 1 μM free GTI-2040, LPs or Tf-LPs containing scrambled ODNs, repsectively (Figure S2 in the Supporting Information). Upon increasing the ODN concentration to 3 μM, we showed up to 90 ± 2% R2 downregulation in cells treated with GTI-2040-Tf-LPs, while 84 ± 2% R2 downregulation was induced with nontargeted

(21) MacGillivray, R. T.; Mendez, E.; Shewale, J. G.; Sinha, S. K.; Lineback-Zins, J.; Brew, K. The primary structure of human serum transferrin. The structures of seven cyanogen bromide fragments and the assembly of the complete structure. *J. Biol. Chem.* **1983**, *258*, 3543–3553.

(22) Bailey, S.; Evans, R. W.; Garratt, R. C.; Gorinsky, B.; Hasnain, S.; Horsburgh, C.; Jhoti, H.; Lindley, P. F.; Mydin, A.; Sarra, R.; Watson, J. L. Molecular structure of serum transferrin at 3.3-Å resolution. *Biochemistry* **1988**, *27*, 5804–5812.

(23) Mattia, E.; Rao, K.; Shapiro, D. S.; Sussman, H. H.; Klausner, R. D. Biosynthetic regulation of the human transferrin receptor by desferrioxamine in K562 cells. *J. Biol. Chem.* **1984**, *259*, 2689–2692.

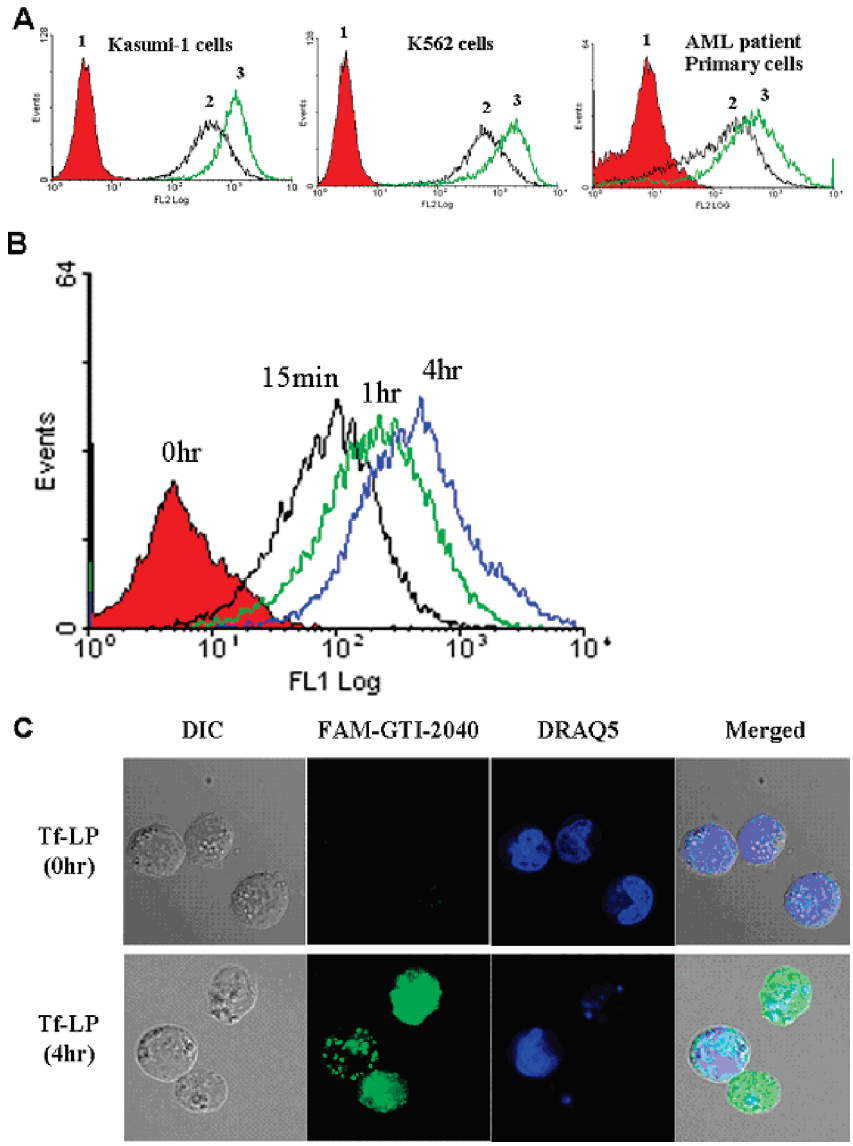

Figure 3. (A) Flow cytometry study of TfR expression: (1) cells stained with PE-isotype; (2) cells stained with PE-anti-TfR; (3) cells stained with PE-anti-TfR after DFO pretreatment at 30 μM concentration for 18 h. (B) The time-dependent uptake of FAM-GTI-2040-Tf-LPs by AML cells. Kasumi-1 cells were treated with 1 μM FAM-GTI-2040-Tf-LPs at 37 °C for various incubation periods, washed twice in PBS and analyzed by flow cytometry. (C) Confocal microscopy images were used to compare the uptake and subcellular distribution of FAM-GTI-2040 delivered by Tf-LPs (1 μM) after 0 h and 4 h incubation respectively. DIC: differential interference contrast (bright field) images. Green fluorescence of FAM-GTI-2040 and blue fluorescence of DRAQ5 were acquired, and merged images were produced.

GTI-2040-LPs (Figure 4A). In contrast, treatment with 3 μM Tf-LPs containing scrambled ODNs only caused 14 $\pm$ 3% R2 downregulation. A similar trend of R2 mRNA downregulation was observed (Figure S3 in the Supporting Information). These data support more efficient cellular delivery of the antisense and downregulation of the target by GTI-2040-Tf-LPs compared to nontargeted LPs.

Despite the more efficient delivery of GTI-2040 by Tf-LPs, only 23% target downregulation was observed at 1 μM concentration. Nevertheless, we showed that GTI-2040 delivery by Tf-LPs was further enhanced by pretreatment with 30 μM DFO for at least 18 h (Figure 4B). As shown in Figure 4B, at 1 μM GTI-2040-Tf-LPs concentration, DFO pretreatment improved R2 downregulation (49 $\pm$ 4%) in Kasumi-1 cells compared to the samples without DFO pretreatment (17 $\pm$ 3%). At 3 μM GTI-2040-Tf-LP concentration, DFO pretreatment also improved the R2 downregulation from 88 $\pm$ 1% to 94 $\pm$ 1%.

3.5. R2 Downregulation by GTI-2040-Tf-LPs in AML Patient Primary Cells. GTI-2040-Tf-LPs dose-dependent R2 downregulation was proven in blasts collected from two AML patients treated at our institution (Figure 5 and Figure S4 in the Supporting Information). Blasts from a third patient were used to conduct studies of the enhancing

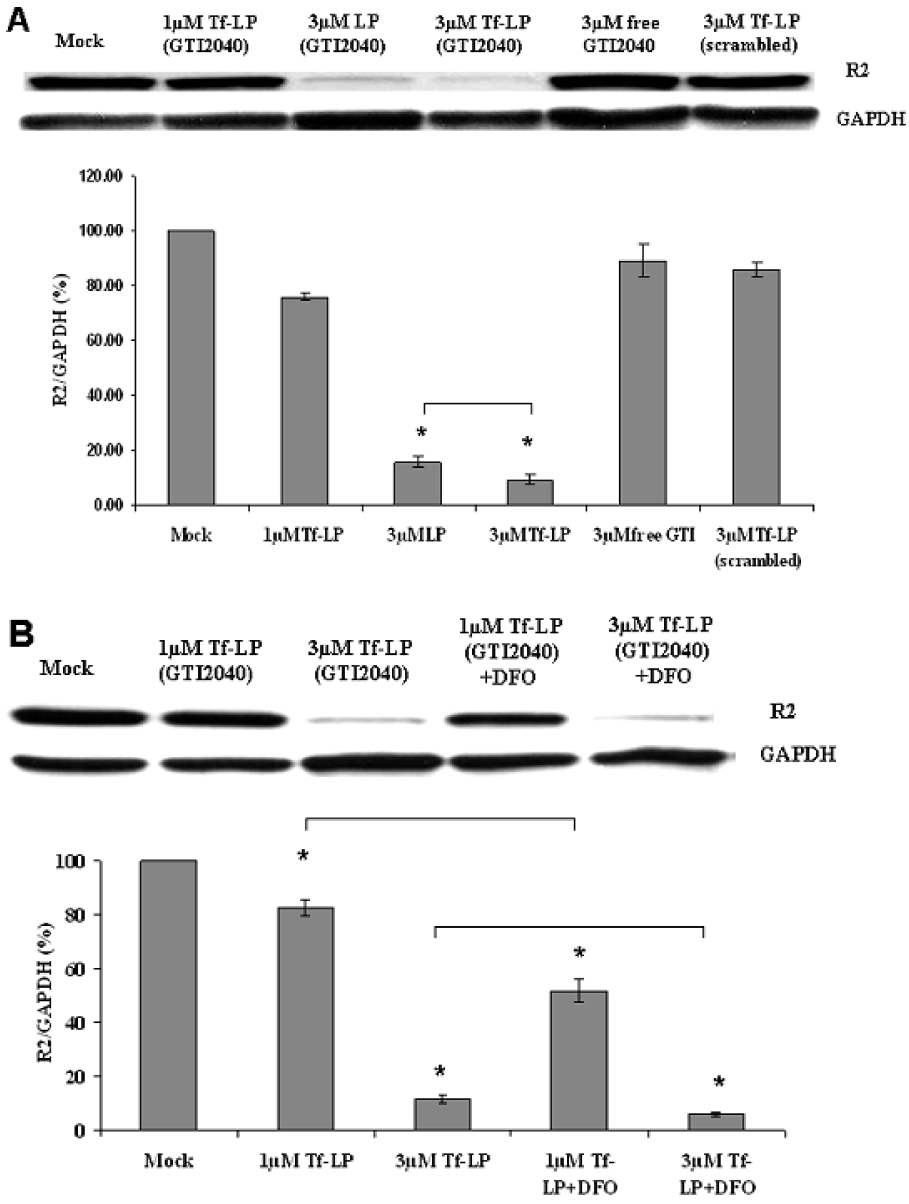

Figure 4. R2 downregulation in Kasumi-1 AML cells under various conditions after 48 h. Every sample was compared with Mock. Each column reflects the average of at least three independent experiments. The standard deviation is elucidated with an error bar. * indicates these data are statistically different from each other. (A) Upper panel shows the representative Western blot image. Lower panel shows the average densitometry data. (B) Improved R2 downregulation with DFO pretreament at 30 μM for 18 h. Upper panel shows representative Western blot image. Lower panel shows the average densitometry data.

effect of DFO (Figure 5B). We showed that DFO, which by itself did not have any effect on R2 expression levels under current pretreatment conditions, enhanced the antisense activity of 1 μM and 3 μM GTI-2040-Tf-LPs (Figure 5B). DFO pretreatment did not have any effect on R2 expression in cell treated with scrambled-Tf-LPs.

The expression levels of TfR on AML primary cells from patients 1−3 were analyzed using flow cytometry (Figure S5 in the Supporting Information). Patient 3 has a lower level of expression of TfR, which may explain the reduced response to Tf-LP treatment in the absence of pre-exposure to DFO.

3.6. GTI-2040-Tf-LPs Improved the Chemosensitivity of AML Cells to Ara-C. A phase I clinical trial in AML at OSU has demonstrated that GTI-2040 and high-dose Ara-C can be coadministered safely and showed reduction of R2 and promising clinical response.[7] In the current study, we sought to demonstrate that improved delivery of GTI-2040 results in an increased sensitivity to Ara-C in AML cells. We treated Kasumi-1 cells with GTI-2040-Tf-LPs, free GTI-2040 or Scrambled-Tf-LPs, followed by cell exposure to various Ara-C concentrations. Cell proliferation and survival were then evaluated by MTS assay. As shown in Figure 6, at concentration as low as 1 μM, only GTI-2040-Tf-LPs

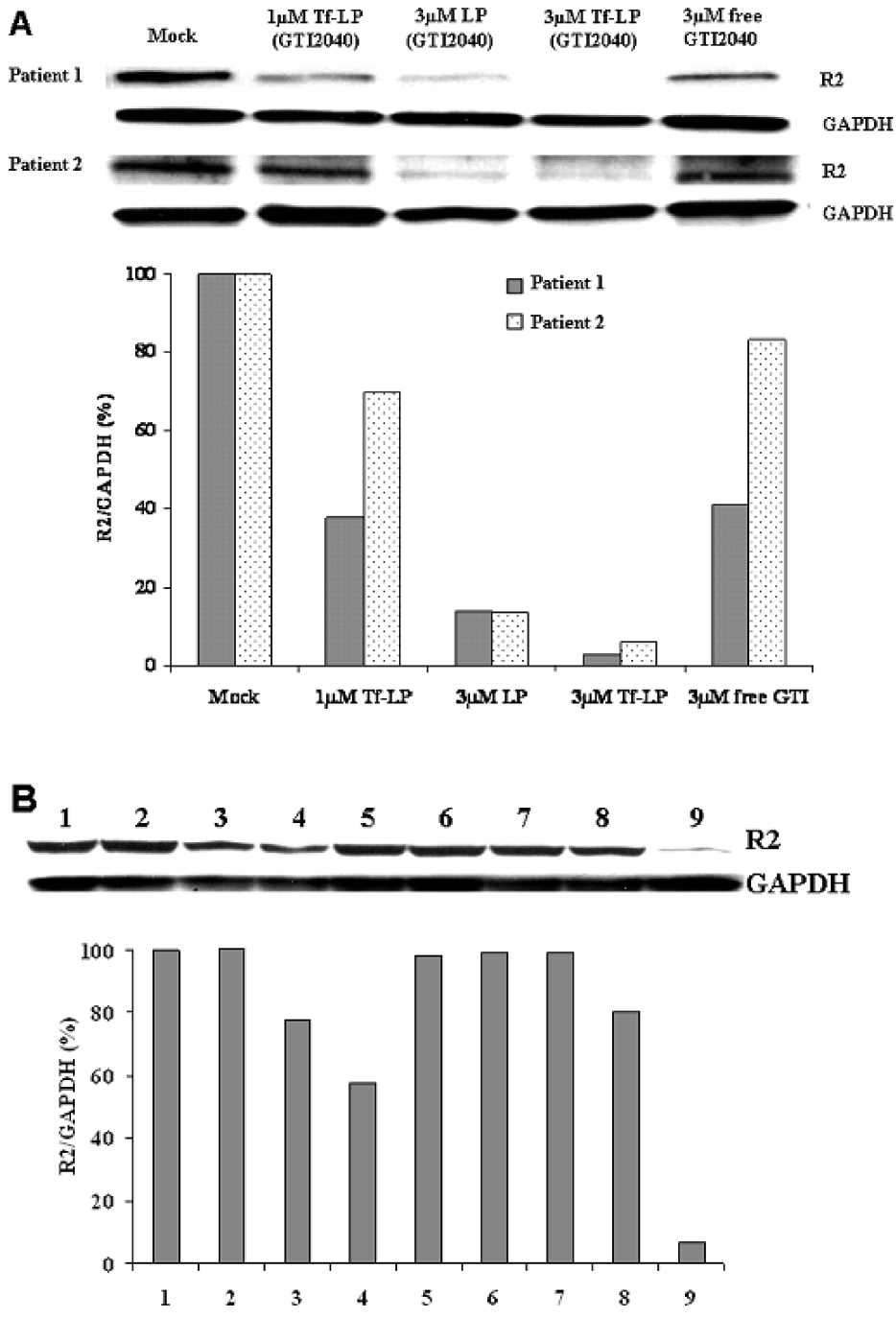

Figure 5. R2 downregulation in AML patient primary cells after 48 h. Every sample was compared with Mock. (A) Upper panel shows the Western blot image. Lower panel shows the densitometry data. (B) Improved R2 downregulation with DFO pretreated AML patient primary cells from patient 3 after 48 h: (1) Mock, (2) 1 μM Tf-LPs (GTI-2040), (3) 3 μM LPs (GTI-2040), (4) 3 μM Tf-LPs (GTI-2040), (5) 3 μM free GTI-2040, (6) 3 μM Tf-LPs (Scrambled), (7) cells treated with DFO treatment as control, (8) 1 μM Tf-LPs (GTI-2040) + DFO pretreatment, and (9) 3 μM Tf-LPs (GTI-2040) + DFO pretreatment. In samples 7, 8 and 9, cells were pretreated with 30 μM DFO for 18 h before the GTI-2040-Tf-LP treatment. Upper panel shows the Western blot image. Lower panel shows the densitometry data.

could sensitize Kasumi-1 cells to Ara-C, with the IC_{50} of Ara-C decreased by 5-fold from 47.69 nM to 9.05 nM. Free GTI-2040 and Tf-LPs containing scrambled ODNs had no chemosensitization effect, consistent with the trend observed for R2 downregulation (Figure 4A).

4. Discussion

The goal of our work is to develop formulations capable of improving targeted delivery of ODNs to specific populations of malignant cells, thereby enhancing their clinical efficacy and reduce their side effects in normal tissue. Herein,

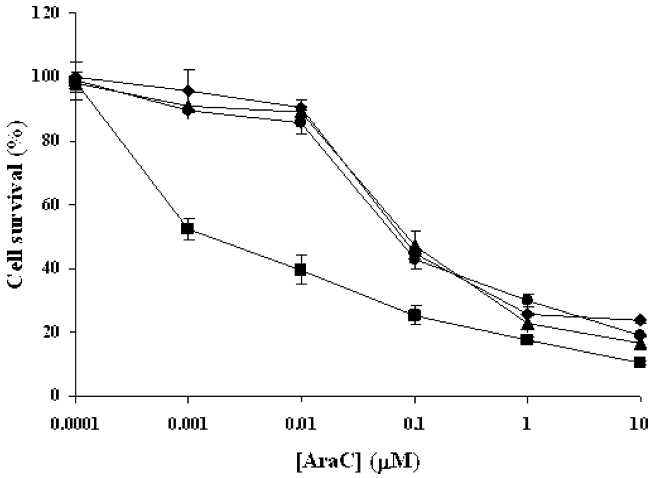

Figure 6. Chemosensitization of Kasumi-1 cells to Ara-C mediated by GTI-2040-Tf-LPs. Cells were treated with buffer (as Mock), GTI-2040-Tf-LPs, free GTI-2040 or Scrambled-Tf-LPs at 1 μM concentration for 4 h, and then the cells were challenged with Ara-C at various concentrations (0.0001−10 μM) for 48 h: (◆) Mock + Ara-C; (■) GTI-2040-Tf-LPs + Ara-C; (▲) free GTI-2040 + Ara-C; and (●) Scrambled-Tf-LPs + Ara-C. Each point reflects the average of at least three independent experiments. Error bars indicate standard deviations.

we report Tf-LPs efficiently delivered GTI-2040 into AML cells, downregulated R2, and chemosensitized the cells to Ara-C. These effects were highly sequence specific and formulation dependent, as free GTI-2040 or Tf-LPs containing scrambled ODNs showed much less or no antisense activity. Importantly, we showed that the cytotoxicity against AML cells of our novel compound was due to the delivered antisense, GTI-2040, and not to the target-LP formulation by itself.

Overcoming the delivery obstacle is the greatest challenge for ODNs in clinical application.[24,25] A variety of vehicles have been developed to facilitate delivery of ODNs.[26] Polymers and lipids are two major classes of materials commonly used for condensing DNA/ODN into nanoparticles by forming polymer−DNA complexes (polyplexes),[27−31] lipid−DNA/ODN complexes (lipoplexes),[32−35] and lipid−polymer−DNA/ODN ternary complexes (LPs),[36−38] respectively. In this study, we developed LPs for GTI-2040 ODN delivery. The advantage of LPs is that DNA/ODN is optimally stabilized via complex with the cationic polymer which has high charge density. Furthermore, LPs are stabilized with a lipid coating that enables flexible surface modifications such as PEGylation to promote colloidal stability, long plasma half-life, and enhanced permeability and retention (EPR) effect-mediated delivery. Finally, targeting ligands such as antibodies (e.g., anti-CD52),[14,15,39] Tf,[17] and folate[38,40] have been conjugated to LPs to achieve specific delivery in tumor tissues expressing the corresponding antigens or receptors. Based on these properties, the LP formulation platform appears to be a promising strategy for engineering targeted multifunctional nanoparticles for ODN delivery, such as GTI-2040, and overcoming the delivery problems hitherto faced by these compounds.

(24) Lebedeva, I.; Stein, C. A. Antisense oligonucleotides: promise and reality. *Annu. Rev. Pharmacol. Toxicol.* **2001**, *41*, 403–419.
(25) Fattal, E.; Couvreur, P.; Dubernet, C. "Smart" delivery of antisense oligonucleotides by anionic pH-sensitive liposomes. *Adv. Drug Delivery Rev.* **2004**, *56*, 931–946.
(26) Patil, S. D.; Rhodes, D. G.; Burgess, D. J. DNA-based therapeutics and DNA delivery systems: a comprehensive review. *AAPS J.* **2005**, *7*, E61-E77.
(27) Wagner, E.; Zenke, M.; Cotten, M.; Beug, H.; Birnstiel, M. L. Transferrin-polycation conjugates as carriers for DNA uptake into cells. *Proc. Natl. Acad. Sci. U.S.A.* **1990**, *87*, 3410–3414.
(28) Boussif, O.; Lezoualc'h, F.; Zanta, M. A.; Mergny, M. D.; Scherman, D.; Demeneix, B.; Behr, J. P. A versatile vector for gene and oligonucleotide transfer into cells in culture and in vivo: polyethylenimine. *Proc. Natl. Acad. Sci. U.S.A.* **1995**, *92*, 7297–7301.
(29) Tang, M. X.; Szoka, F. C. The influence of polymer structure on the interactions of cationic polymers with DNA and morphology of the resulting complexes. *Gene Ther.* **1997**, *4*, 823–832.
(30) Leong, K. W.; Mao, H. Q.; Truong-Le, V. L.; Roy, K.; Walsh, S. M.; August, J. T. DNA-polycation nanospheres as non-viral gene delivery vehicles. *J. Controlled Release* **1998**, *53*, 183–193.
(31) Roy, K.; Mao, H. Q.; Huang, S. K.; Leong, K. W. Oral gene delivery with chitosan--DNA nanoparticles generates immunologic protection in a murine model of peanut allergy. *Nat. Med.* **1999**, *5*, 387–391.
(32) Nabel, G. J.; Nabel, E. G.; Yang, Z. Y.; Fox, B. A.; Plautz, G. E.; Gao, X.; Huang, L.; Shu, S.; Gordon, D.; Chang, A. E. Direct gene transfer with DNA-liposome complexes in melanoma: expression, biologic activity, and lack of toxicity in humans. *Proc. Natl. Acad. Sci. U.S.A.* **1993**, *90*, 11307–11311.
(33) Caplen, N. J.; Alton, E. W.; Middleton, P. G.; Dorin, J. R.; Stevenson, B. J.; Gao, X.; Durham, S. R.; Jeffery, P. K.; Hodson, M. E.; Coutelle, C.; Huang, L.; Porteous, D. J.; Williamson, R.; Geddes, D. M. Liposome-mediated CFTR gene transfer to the nasal epithelium of patients with cystic fibrosis. *Nat. Med.* **1995**, *1*, 39–46.
(34) Liu, F.; Yang, J.; Huang, L.; Liu, D. New cationic lipid formulations for gene transfer. *Pharm. Res.* **1996**, *13*, 1856–1860.
(35) Wilson, A.; Zhou, W.; Champion, H. C.; Alber, S.; Tang, Z. L.; Kennel, S.; Watkins, S.; Huang, L.; Pitt, B.; Li, S. Targeted delivery of oligodeoxynucleotides to mouse lung endothelial cells in vitro and in vivo. *Mol. Ther.* **2005**, *12*, 510–518.
(36) Pelisek, J.; Gaedtke, L.; DeRouchey, J.; Walker, G. F.; Nikol, S.; Wagner, E. Optimized lipopolyplex formulations for gene transfer to human colon carcinoma cells under in vitro conditions. *J. Gene Med.* **2006**, *8*, 186–197.
(37) Gao, X.; Huang, L. Potentiation of cationic liposome-mediated gene delivery by polycations. *Biochemistry* **1996**, *35*, 1027–1036.
(38) Lee, R. J.; Huang, L. Folate-targeted, anionic liposome-entrapped polylysine-condensed DNA for tumor cell-specific gene transfer. *J. Biol. Chem.* **1996**, *271*, 8481–8487.
(39) Leserman, L. D.; Machy, P.; Barbet, J. Cell-specific drug transfer from liposomes bearing monoclonal antibodies. *Nature* **1981**, *293*, 226–228.
(40) Lee, R. J.; Low, P. S. Delivery of liposomes into cultured KB cells via folate receptor-mediated endocytosis. *J. Biol. Chem.* **1994**, *269*, 3198–3204.

In our work, protamine sulfate, a clinically used polycationic peptide, was used as a good candidate of biodegradable cationic polymers. It can bind ODNs to form a compact structure via electrostatic interactions, and has been shown to facilitate DNA delivery.[41] Lipid bilayers composed of CHEMS, a pH-sensitive lipid, and DOPE, a fusogenic lipid, are known to undergo a transition from lamellar to hexagonal II phase at low pH, which can destabilize endosomes through proximity following endocytosis.[25] Therefore, LPs with these lipids are capable of releasing their contents in response to acidic pH within the endosomal system while remaining stable in plasma, thus improving the cytoplasmic delivery of ODNs after endocytosis. Tf, an 80 kDa iron-transporting glycoprotein, can be efficiently taken up by cells via TfR-mediated endocytosis.[21,22] TfR is considered a good target for cancer-specific delivery, as it is commonly overexpressed on cancer cells including AML[12,13] compared to normal cells. This was confirmed in our study (Figure 3A). In addition, Tf is less immunogenic and more cost-effective than monoclonal antibodies, and easy to handle and store.[42]

The detailed structure of LP nanoparticles was studied with Cryo-TEM, indicating several coexisting structures, including onion-like LPs (Figure 2B), in which the ODNs were condensed between two adjacent lipid bilayers, empty liposomes, and amorphous complexes of protamine/ODN. Although the current LP structure is nonuniform, we are currently developing better LP synthesis methods, such as microfluidic focusing,[43] to improve the uniformity of the nanoparticle size and structure, as well as increase ODN loading with less lipids and condensing agents for better transfection efficiency and less cytotoxicity.

The marked decrease in R2 levels in cells treated with 3 μM untargeted LPs might be due to treatment with a large number of LPs. In the future, targeted LPs with a higher ODN loading and hence needing to treat cells with a lower concentration of LPs may address this. Nevertheless, another important point of Figures 4A and 5A is that, at the same concentration (3 μM), Tf-LPs performed better than untargeted LPs.

DFO is an iron chelator known to increase TfR expression.[23] This compound is already in the clinic and used for the treatment of iron overload.[44] Therefore, we would not expect any unanticipated toxicity, should it be incorporated in combination with GTI-2040-Tf-LPs in clinical programs for AML patients. Although DFO treatment may also increase the TfR expression level on normal cells, it is possible that cancer cells are more sensitive to this compound as rapidly dividing cells have an increased demand for iron.[45] In the present study, pretreatment of DFO increased TfR expression on both AML cell lines and patient primary cells, and improved the efficacy of GTI-2040-Tf-LPs. This implied that pretreatment of DFO may also improve the targeted delivery and efficacy of GTI-2040 delivered by Tf-LPs in a clinical situation. However, whether or not DFO may increase side effects on normal tissue in patients treated with GTI-2040-Tf-LPs is currently unknown and should be one of primary end points of analysis in future clinical trials.

Because of early onset of mechanisms of resistance, AML patients are commonly treated with a multidrug chemotherapy regimen. We combined here GTI-2040 with Ara-C, which represents the backbone for both upfront and salvage regimen in AML. The rationale for this combination is that the metabolite of Ara-C, Ara-CTP, incorporates into DNA and terminates DNA chain elongation by competing with the endogenous dCTP derived from RNR-mediated nucleotide reduction.[46−49] It is expected that downregulation of the R2 subunit of RNR by GTI-2040 decreases the endogenous levels of dCTP and further increases the Ara-CTP/dNTP ratio thereby augmenting DNA incorporation of Ara-CTP.[8] This combination has been studied in the phase I clinical trial at OSU, leading to promising results.[7] However, the in vivo downregulation of R2 in patients treated on this trial was only $\leq$50%. Therefore, to attain a more efficient R2 downregulation and further enhance the therapeutic efficacy of GTI-Ara-C combination, we improved the intracellular delivery of GTI-2040 by Tf-LPs. At a concentration of GTI-2040-Tf-LP as low as 1 μM, it could sensitize AML cells to Ara-C, with the IC_{50} of Ara-C decreased by 5-fold, thereby further supporting the hypothesis that this combination is effective and needs to be further studied in clinical trials.

(41) Sorgi, F. L.; Bhattacharya, S.; Huang, L. Protamine sulfate enhances lipid-mediated gene transfer. *Gene Ther.* **1997**, *4*, 961–968.

(42) Sapra, P.; Allen, T. M. Ligand-targeted liposomal anticancer drugs. *Prog. Lipid Res.* **2003**, *42*, 439–462.

(43) Koh, C. G.; Zhang, X.; Liu, S.; Golan, S.; Yu, B.; Yang, X.; Guan, J.; Jin, Y.; Talmon, Y. ; Muthasamy, N.; Chan, K. K.; Bryd, J. C.; Lee, R. J.; Marcucci, G. ; Lee, L. J. Delivery of Antisense Oligodeoxyribonucleotide Lipopolyplex Nanoparticles Assembled by Microfluidic Hydrodynamic Focusing. *J. Controlled Release* **2009**, doi: 10.1016/j.jconrel.2009.08.019.

(44) Ault, P.; Jones, K. Understanding iron overload: screening, monitoring, and caring for patients with transfusion-dependent anemias. *Clin. J. Oncol. Nurs.* **2009**, *13*, 511–517.

(45) Dayani, P. N.; Bishop, M. C.; Black, K.; Zeltzer, P. M. Desferoxamine (DFO)--mediated iron chelation: rationale for a novel approach to therapy for brain cancer. *J. Neurooncol.* **2004**, *67*, 367–377.

(46) Fan, H.; Villegas, C.; Wright, J. A. Ribonucleotide reductase R2 component is a novel malignancy determinant that cooperates with activated oncogenes to determine transformation and malignant potential. *Proc. Natl. Acad. Sci. U.S.A.* **1996**, *93*, 14036–14040.

(47) Fan, H.; Villegas, C.; Huang, A.; Wright, J. A. The mammalian ribonucleotide reductase R2 component cooperates with a variety of oncogenes in mechanisms of cellular transformation. *Cancer Res.* **1998**, *58*, 1650–1653.

(48) Tanaka, H.; Arakawa, H.; Yamaguchi, T.; Shiraishi, K.; Fukuda, S.; Matsui, K.; Takei, Y.; Nakamura, Y. A ribonucleotide reductase gene involved in a p53-dependent cell-cycle checkpoint for DNA damage. *Nature* **2000**, *404*, 42–49.

(49) Hakansson, P.; Hofer, A.; Thelander, L. Regulation of mammalian ribonucleotide reduction and dNTP pools after DNA damage and in resting cells. *J. Biol. Chem.* **2006**, *281*, 7834–7841.

5. Conclusions

In summary, targeted LPs with high ODN encapsulation efficiency have been developed in this study. The GTI-2040-Tf-LPs effectively downregulated R2 expression in AML cell lines and AML patient primary cells, and chemosensitized AML cells toward Ara-C. Further preclinical evaluation and potential clinical trials for this promising formulation of GTI-2040 are warranted.

Acknowledgment. This work was supported by NIH Grant R01CA135243 (R.J.L., G.M. and L.J.L.) and NSF Grant EEC-0425626 (L.J.L.). We thank Lorus Therapeutics Inc. for providing the GTI-2040 ODN used in this study and Dr. Peter Murray for helpful input during manuscript preparation.

Supporting Information Available: Figures S1 through S5 depicting agarose gel electrophoresis of GTI-2040, Western blot result for R2 downregulation in Kasumi-1 AML cells, qRT-PCR results of *R2* mRNA downregulation in Kasumi-1 AML cells, qRT-PCR results for *R2* mRNA downregulation in AML patient primary cells and flow cytometry study of TfR expression level on the patient cell surface. This material is available free of charge via the Internet at http://pubs.acs.org.

MP900205R